Fusion of heavy ions by means of the Langevin equation

K. Mahboub,* A. Zerarka,[1] and V. G. Foester[1]
Département de Physique Nucléaire, Université Med Khider, B P 145 Biskra 07000, Algeria
(Received 6 December 2003; published 29 June 2005)

The Langevin equation was used to describe fusion dynamics in two systems, ^{64}Ni+^{100}Mo and ^{64}Ni+^{96}Zr. The corresponding fusion cross sections were calculated for different energies, and the mean angular momentum and its dependence on energy were also obtained. We were able to reproduce experimental fusion cross sections at high energies with the one-body dissipation mechanism. Attention was focused on the fusion barrier calculated with the Yukawa-plus-exponential method.

DOI: 10.1103/PhysRevC.71.064609 PACS number(s): 25.60.Pj, 05.10.Gg, 51.10.+y

I. INTRODUCTION

The application of nonequilibrium statistical approaches (transport equations) to describe heavy ion collisions starts with the discovery of relaxation phenomena and diffusion processes in deep-inelastic collisions (DIC). The concepts of friction and diffusion were incorporated into the equations of motion to estimate statistically the role of the intrinsic degrees of freedom involved in the reaction. It is also assumed that those degrees of freedom equilibrate faster than the collective ones. This allows us to handle them as a heat bath of a temperature T function of time. Fission [1], fusion [2], and DIC [3] were treated at the same level by means of the Langevin or Fokker-Planck equations. In the case of fusion, the presence of friction forces explain why the system needs an extra push of energy to overcome the static fusion barrier. A trajectory with friction forces loses energy and has a smaller probability of entering into the nuclear pocket, which leads to a reduction of the fusion cross section contrary to the prediction of the classical model.

The purpose of this work is to account for the experimental cross sections and mean angular momentum of the fused system for medium nuclei over a wide range of energy. We have calculated the ingredients from realistic models. This allows us to determine the origin of the discrepancy between theoretical calculations and experimental data.

II. INPUT PARAMETERS OF THE MODEL

A. Shape parametrization

Since the two colliding nuclei show in general asymmetry, we need a parametrization that accounts for the asymmetry parameter. In previous works, we find the Blocki and Swiatecki [4] parametrization was often considered. In this work we have opted for the funny-hills parametrization [5] or the so-called $(\overline{c}, h, \alpha)$ parametrization because of its simplicity. For axially symmetric shapes in cylindrical coordinates

$$z = C\,(u - \bar{u})\,, \qquad \varrho = C v_s, \tag{1}$$

u and v_s are the corresponding dimensionless coordinates, $\bar{u}$ is the position of the center of mass of the system, and C is a scaling factor determined by the volume conservation condition.

The shape function v_s is given by

$$v_s^2 = \begin{cases} (1-u^2)(A + Bu^2 + \alpha u), & B > 0, \\ (1-u^2)(A + \alpha u)e^{-qu^2}, & B < 0, \end{cases} \tag{2}$$

$$q = -B\overline{c}^3, \tag{3}$$

where $\overline{c} = C/R_0$, R_0 is the nuclear radius of the compound system, and A, B, α are the independent deformation parameters.

For connected shapes and from volume conservation, we have

$$q = -\frac{5B}{5A + B}, \qquad B > 0, \tag{4}$$

and

$$\frac{-4B}{3A} = e^{-q} + \sqrt{\pi q}\left(1 - \frac{1}{2q}\right)\mathrm{erf}(\sqrt{q}), \quad B < 0, \tag{5}$$

where $\mathrm{erf}(x)$ is the error function.

However, it is useful to use the parameters $\overline{c}$, h, α where h is defined for the two cases by

$$B = 2h + \frac{(\overline{c} - 1)}{2}, \tag{6}$$

where $\overline{c}$ is the half length of the longer axis of the nucleus in units of R_0, h describes the variation of the thickness of the neck radius, and α denotes the right-left asymmetry of the nucleus.

We define the collective relative coordinate, which is the distance between the centers of mass of the two colliding nuclei (independent of α), as

$$\varrho_{\mathrm{c.m.}} = 2\overline{c}\frac{\left(\frac{A}{2} + \frac{B}{6}\right)}{\frac{4}{3}\left(A + \frac{B}{5}\right)}, \quad B > 0, \tag{7}$$

$$\varrho_{\mathrm{c.m.}} = 2\overline{c}\frac{e^{-q} + \frac{1}{q}(e^{-q} - 1)}{e^{-q} + \sqrt{\pi q}\,\mathrm{erf}(\sqrt{q})\left(1 - \frac{1}{2q}\right)}, \quad B < 0. \tag{8}$$

*Author to whom correspondence should be addressed. E-mail: abzerarka@yahoo.fr

B. Potential energy

The conservation energy equation can be expressed as

$$M_1(0)c^2 + M_2(0)c^2 + E_{\text{c.m.}} = M(r)c^2 + \frac{P_r^2}{2\mu} + \frac{(L/r)^2}{2\mu} + E^*. \tag{9}$$

$M_i(0)$ denotes the nuclear mass of the spherical nucleus i, $M(r)$ is the nuclear mass of the whole system at distance r, $E_{\text{c.m.}}$ is the center-of-mass energy, P_r is the relative momentum, L is the relative angular momentum, E^* is the excitation energy of the system, and μ is the reduced mass parameter.

$$M_i(0) = M_i^{\text{LD}}(0) + M_{\text{shell},i}(0), \tag{10}$$

where M_i^{LD} is the liquid drop part and $M_{\text{shell},i}$ is the shell correction to the liquid drop part.

$$M_i^{\text{LD}}(0)c^2 = N_i M_n c^2 + Z_i M_p c^2 + E_{\text{Coul},i}(0) + E_{N,i}(0), \tag{11}$$

where N_i, Z_i, c, $E_{\text{Coul},i}$, and $E_{N,i}$ are the neutron number, atomic number, light celerity, Coulomb energy, and nuclear energy of the nucleus i, respectively.

$$M(r)c^2 = NM_n c^2 + ZM_p c^2 + E_{\text{Coul}}(r) + E_N(r) + \overline{M}_{\text{shell}}(r), \tag{12}$$

from (9) we can get

$$\begin{aligned} E_{\text{c.m.}} &= E_N(r) - E_{N,1}(0) - E_{N,2}(0) + E_{\text{Coul}}(r) \\ &\quad - E_{\text{Coul},1}(0) - E_{\text{Coul},2}(0) + \overline{M}_{\text{shell}}(r) \\ &\quad - M_{\text{shell},1}(0) - M_{\text{shell},2}(0) + \frac{P_r^2}{2\mu} + \frac{(l/r)^2}{2\mu} + E^* \\ &= V_N + V_{\text{Coul}} + V_{\text{shell}} + \frac{P_r^2}{2\mu} + \frac{(l/r)^2}{2\mu} + E^*, \end{aligned} \tag{13}$$

where we defined from the above equation the nuclear, Coulomb, and shell interaction potentials.

The nuclear potential energy is the short-range force surface energy using a Yukawa-plus-exponential (YE) form of interaction [6], that is,

$$E_{\text{YE}}(r) = \frac{E^0_{s,\text{YE}}}{8\pi^2 a^4 R_0^2} \int d^3\vec{r}'' \int d^3\vec{r}' \times \left(2 - \frac{|\vec{r}'' - \vec{r}'|}{a}\right) \frac{\exp\left(-\frac{|\vec{r}'' - \vec{r}'|}{a}\right)}{\frac{|\vec{r}'' - \vec{r}'|}{a}}, \tag{14}$$

where the integration is taken for the configuration defined by r or $\rho_{\text{c.m.}}$. $R_0 = r_0 A_c^{1/3}$, $E^0_{s,\text{YE}} = C_s A_c^{2/3}$, $C_s = a_s[1 - k_s(\frac{N-Z}{A_c})^2]$, $a_s = 21.7$ MeV, $k_s = 3$, $r_0 = 1.18$ fm, $a = 0.65$ fm, A_c is the mass of the compound nucleus, and the subscript N in the nuclear potential energy is replaced by YE.

The Coulomb part of energy is evaluated by the introduction of a charge distribution ϱ_{ch} assumed uniform.

$$E_{\text{Coul}}(r) = \frac{\varrho_{\text{ch}}}{2} \int d^3\vec{r}'' \int d^3\vec{r}' |\vec{r}'' - \vec{r}'|^{-1}. \tag{15}$$

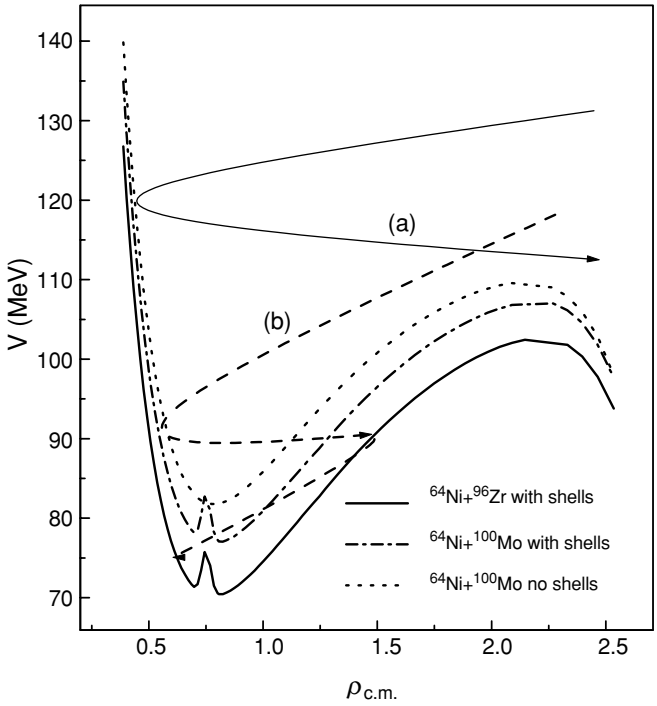

FIG. 1. Potential energy as function of c.m. dimensionless relative distance for ^{64}Ni+^{100}Mo with and without shell effects and for ^{64}Ni+^{96}Zr with shell effects. Trajectory (a) (solid line) corresponds to weak friction and leads to scattering; trajectory (b) (dashed line) is a fusion event.

We can see from the above definitions that V_N, $V_{\text{Coul}} \longrightarrow 0$, when $r \longrightarrow \infty$ as it would be.

The shell potential V_{shell} must tend to $M_{\text{shell},1}(0) + M_{\text{shell},2}(0)$ when $r \longrightarrow \infty$, i.e, when the neck radius between the two nuclei is zero. We define a variable $0 \leqslant \beta \leqslant 1$ proportional to the neck radius as in Ref. [7] such as

$$\overline{M}_{\text{shell}}(r) = \beta M_{\text{shell}}(r) + (1 - \beta)[M_{\text{shell},1}(0) + M_{\text{shell},2}(0)], \tag{16}$$

and the potential shell correction energy becomes

$$V_{\text{shell}} = \beta[M_{\text{shell}}(r) - M_{\text{shell},1}(0) - M_{\text{shell},2}(0)]. \tag{17}$$

The shell correction M_{shell} is due to Myers and Swiatecki and taken from Ref. [8]. The potential energy for the two systems we studied is shown in Fig. 1. The spikes in the potential are due to the shell correction of Meyers-Swiatecki. They show the double well structure of the potential energy.

C. The transport parameters

Several authors use for the evaluation of the inertia tensor, the Werner-Wheeler [9] approximation of an incompressible fluid whose hydrodynamic flow is irrotational. In the presence of viscosity, the flow is no longer irrotational; only at high temperatures, when the viscosity decreases, is the flow nearly irrotational. This is the case, for example, for fission of highly

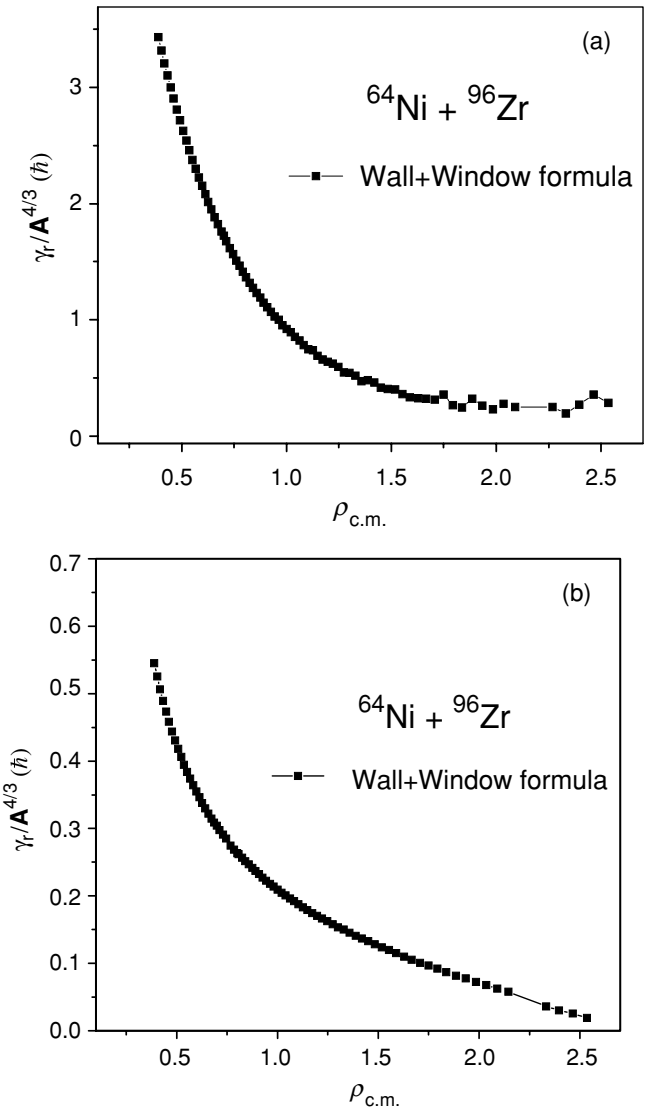

FIG. 2. ^{64}Ni+^{96}Zr system. (a) Radial friction parameter as function of c.m. dimensionless relative distance; (b) tangential friction parameter as function of c.m. dimensionless relative distance.

excited nuclei when the temperature is $T > 2$ MeV. In our case, i.e, fusion, the temperature increases from 0 to 0.96 MeV at $E_{\text{c.m.}} = 127.8$ MeV and from 0 to 1.27 MeV at $E_{\text{c.m.}} = 141.8$ MeV for the system ^{64}Ni+^{100}Mo approximately, which means that the above approximation is not valid. For that we take the reduced mass parameter as a first approximation to the collective mass.

We calculated the friction tensor assuming the one-body dissipation mechanism, i.e., the wall and wall+window formula [10], and we extracted from it the radial (tangential) friction shown in Fig. 2(a) [Fig. 2(b)]. We obtained good results at high energies, and we also used the friction treated by the surface friction model (SFM), but we were not able to reproduce the experimental fusion cross sections simultaneously.

Let us now write the specific wall+ window for the dinuclear regime as

$$\begin{aligned}\dot{Q}_{\text{ww}} = &\frac{3}{4}v_F\rho_m^*\int_{\Sigma A} d\sigma(\dot{n} - D_A)^2 \\ &+ \frac{3}{4}v_F\rho_m^*\int_{\Sigma B} d\sigma(\dot{n} - D_B)^2 \\ &+ \frac{3}{16}v_F\rho_m^*\Delta\sigma(2u_r^2 + u_t^2) + \frac{4}{3}\rho_m^*\frac{v_F}{\Delta\sigma}\dot{V}_A^2, \end{aligned} \tag{18}$$

in which D_A (D_B) is the drift velocity of the fragment A (B), $\Delta\sigma$ the window area, ρ_m^* the nuclear mass density, V_A the volume of fragment A, u_r and u_t the velocity components with respect to relative motion of the fragments, v_F the Fermi velocity, and $\dot{n}$ the surface velocity; the dot denotes the time derivative.

The radial part of the rate energy is

$$\begin{aligned}\dot{Q}_r = &\frac{3}{4}v_F\rho_m^*\int_{\Sigma A} d\sigma(\dot{n} - D_A)^2 \\ &+ \frac{3}{4}v_F\rho_m^*\int_{\Sigma B} d\sigma(\dot{n} - D_B)^2 \\ &+ \frac{3}{16}v_F\rho_m^*\Delta\sigma 2u_r^2 + \frac{4}{3}\rho_m^*\frac{v_F}{\Delta\sigma}\dot{V}_A^2 \\ = &\gamma_r\dot{r}^2, \end{aligned} \tag{19}$$

while the tangential part of the rate energy reads as

$$\dot{Q}_t = \tfrac{3}{16}v_F\rho_m^*\Delta\sigma u_t^2 = \gamma_t r^2\dot{\theta}^2. \tag{20}$$

III. DYNAMICAL EVOLUTION OF THE SYSTEM

The two ions in the touching configuration move toward the equilibrium configuration in an opposite way to fission. In the course of the approaching phase, energy and angular momentum dissipate from collective relative motion into intrinsic degrees of freedom (intrinsic excitation energy and intrinsic angular momentum of the colliding ions). We have two equations of motion: for the radial momentum and for the relative angular momentum. Once the sticking limit is attained ($L_{\text{st}} = 5L_0/7$), there is no longer dissipation of angular momentum, and only dissipation of relative momentum occurs. Since dissipation is followed by fluctuations, we use the Langevin equations, to examine the evolution of our system. We begin with the Lagrange-Hamilton equations, and the classical equations of motion can be derived. The kinetic energy of our system is written as

$$T = \frac{P_r^2}{2\mu} + \frac{1}{2}\mu r^2\dot{\theta}^2, \tag{21}$$

where r is the relative distance between the ions, and θ is the polar angle connected with the tangential motion of the system. Hence, the Rayleigh dissipation function is formulated as

$$R = \tfrac{1}{2}\gamma_r\dot{r}^2 + \tfrac{1}{2}\gamma_t r^2\dot{\theta}^2, \tag{22}$$

the equations of motion read as

$$\begin{cases} \dfrac{dr}{dt} = \dfrac{P_r}{\mu}, \\ \dfrac{dP_r}{dt} = -\dfrac{dV}{dr} - \dfrac{\gamma_r}{\mu}P_r + \dfrac{l^2}{\mu r^3} + L_r(t), \\ \dfrac{d\theta}{dt} = \dfrac{l}{\mu r^2}, \\ \dfrac{dl}{dt} = -\dfrac{\gamma_t}{\mu}l + L_t(t), \end{cases} \tag{23}$$

l is the relative angular momentum, and the forces $L_r(t)$ and $L_t(t)$ are fluctuating forces defined by their first and second moments

$$\begin{aligned} \langle L_i \rangle &= 0, \\ \langle L_i(t)L_i(t') \rangle &= 2D_i\delta(t-t'), \end{aligned} \tag{24}$$

where the subscript i denotes r or t, and D_i is the diffusion parameter related to the friction parameter via the Einstein relation such that

$$\begin{aligned} D_r &= \gamma_r T, \\ D_t &= r^2\gamma_t T, \end{aligned} \tag{25}$$

where T is the nuclear temperature.

The total cross section is calculated by using the Monte Carlo integral procedure [2] with the relations

(1) $l = l_>\sqrt{x}$, this implies $2ldl = l_>^2 dx$, and
(2) $\sigma_F = \sum_l \sigma_l = \sum_l \frac{\pi}{k^2}(2l+1)T_l$, that is,

$$\begin{aligned} \sigma_F &= \sum_l \sigma_l = \frac{\pi}{k^2}\sum_l (2l+1)T_l \cong \frac{\pi}{k^2}\int_0^{l_>} 2lT_l dl \\ &= \frac{\pi}{k^2}l_>^2\int_0^1 T(x)dx = \frac{\pi}{k^2}l_>^2\sum_i \frac{T_i}{N} \\ &= \frac{\pi}{k^2}l_>^2\frac{N_F}{N}, \end{aligned} \tag{26}$$

where N_F is the number of trajectories that lead to fusion for all waves, N is the total number of trajectories, and $l_>$ is the grazing angular momentum.

The spin distributions describing the partial differential cross sections are expressed by

$$\sigma_{l_i} = \frac{\pi}{k^2}(2l_i+1)T_{l_i} = \frac{\pi}{k^2}(2l_i+1)\frac{N_{iF}}{N_i}, \tag{27}$$

where l_i, N_{iF}, and N_i are the angular momentum, the number of fusing, and the total number of trajectories with angular momentum l_i, respectively.

IV. NUMERICAL PROCEDURE

A. Initial conditions

The initial conditions of the problem are the mass numbers A_i, the atomic numbers Z_i, the center-of-mass energy $E_{\text{c.m.}}$, the initial angular momentum l, the initial relative momentum P_0, and the touching point distance r_{sc}. The touching point distance is chosen as the point when the neck is zero. we find $r_{\text{sc}} = 2.53$ in units of R_0. The initial angular momentum is chosen according to $l = l_>\sqrt{x}$, where x is a random number from a uniform distribution ($0 \leqslant x \leqslant 1$), and $l_>$ is the grazing angular momentum calculated by the conservation energy relation when the kinetic energy is set equal to zero.

$$l_> = r_{\text{sc}}\sqrt{2\mu[E_{\text{c.m.}} - V(r_{\text{sc}})]}, \tag{28}$$

the initial relative momentum is deduced from the conservation energy equation as

$$P_0 = -\sqrt{2\mu\left[E_{\text{c.m.}} - V(r_{\text{sc}}) - \frac{(l/r_{\text{sc}})^2}{2\mu}\right]}. \tag{29}$$

B. Integration of the equations of motion

We follow the system along the fusion path by using the time-step integration method. The time step τ is chosen to satisfy the following approximations:

$$\begin{aligned} r_{n+1} &= r_n + \frac{P_n}{\mu}\tau, \\ P_{n+1} &= P_n - \left[\left(\frac{dV}{dr}\right)_{r=r_n} + \beta_r P_n - \frac{l_n^2}{\mu r_n^3}\right]\tau \\ &\quad + \sqrt{D_r(r_n)\tau}\omega_r, \\ \theta_{n+1} &= \theta_n + \frac{l_n}{\mu r_n^2}\tau, \\ l_{n+1} &= l_n - \beta_t l_n\tau + \sqrt{D_t(r_n)\tau}\omega_t, \end{aligned} \tag{30}$$

where ω_t and ω_r are Gaussian-distributed random numbers.

Moreover, the angular momentum dissipated possesses a maximum value calculated by the sticking limit $\Delta L = \frac{2}{5}L_i$, and the energy dissipated is entirely transformed into intrinsic excitation energy provided by the Fermi gas model $E^* = \frac{A}{8}T^2$.

V. RESULTS AND CONCLUSIONS

The results for the systems ^{64}Ni+^{96}Zr and ^{64}Ni+^{100}Mo are presented in Figs. 3(a) and 3(b), respectively. The experimental data are from [11] and [12], respectively. Fusion cross sections were calculated for 1000 trajectories including all partial waves. We performed the calculations for 5000 trajectories for one energy and confirmed that the result is almost the same as that obtained using 1000 trajectories. Figures 4(a) and 4(b) report the mean angular momentum vs energy. We can see that while going toward high energies the agreement is very good, especially for fusion cross sections. At low energies, our model overestimated the fusion cross sections and the mean angular momentum, contrary to the case of no fluctuations ($D = 0$) where it underestimated them. We also reduced the value of the diffusion parameter D by a factor of 5 to see the role of fluctuations. The result is again zero events for the energy 132.8 MeV. In our calculations, we used the standard

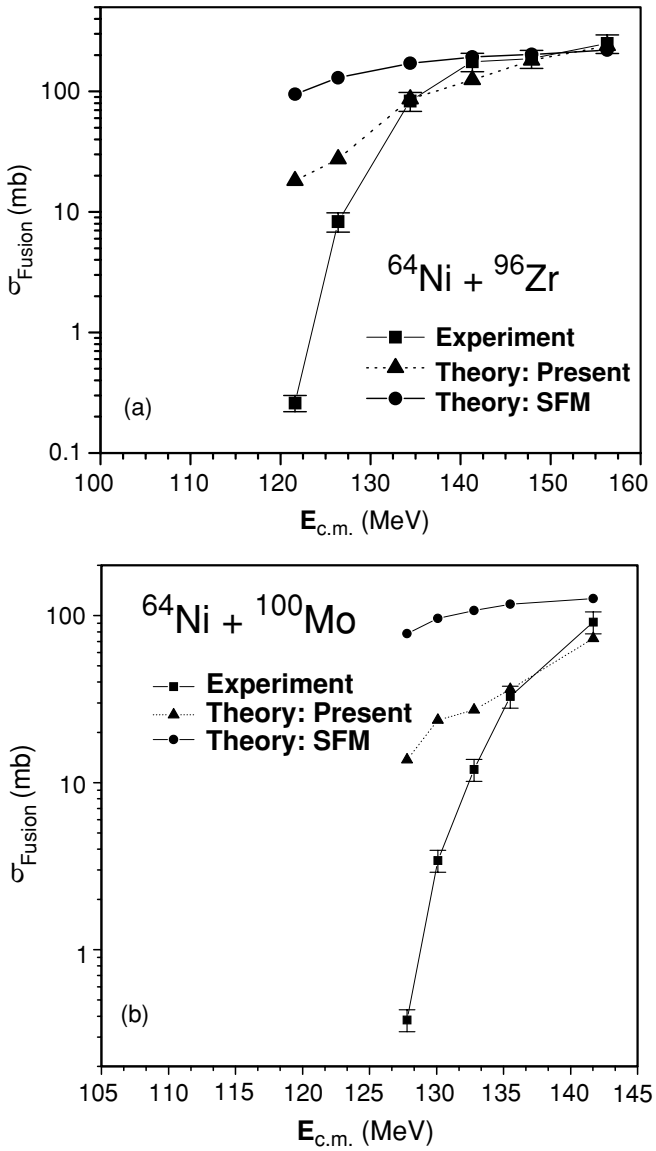

FIG. 3. Fusion cross sections as function of c.m. energy: Comparison with the present theory (one-body dissipation), the SFM theory, and the experiment. (a) For ^{64}Ni+^{96}Zr system with experiment from [11]; (b) for ^{64}Ni+^{100}Mo system with experiment from [12].

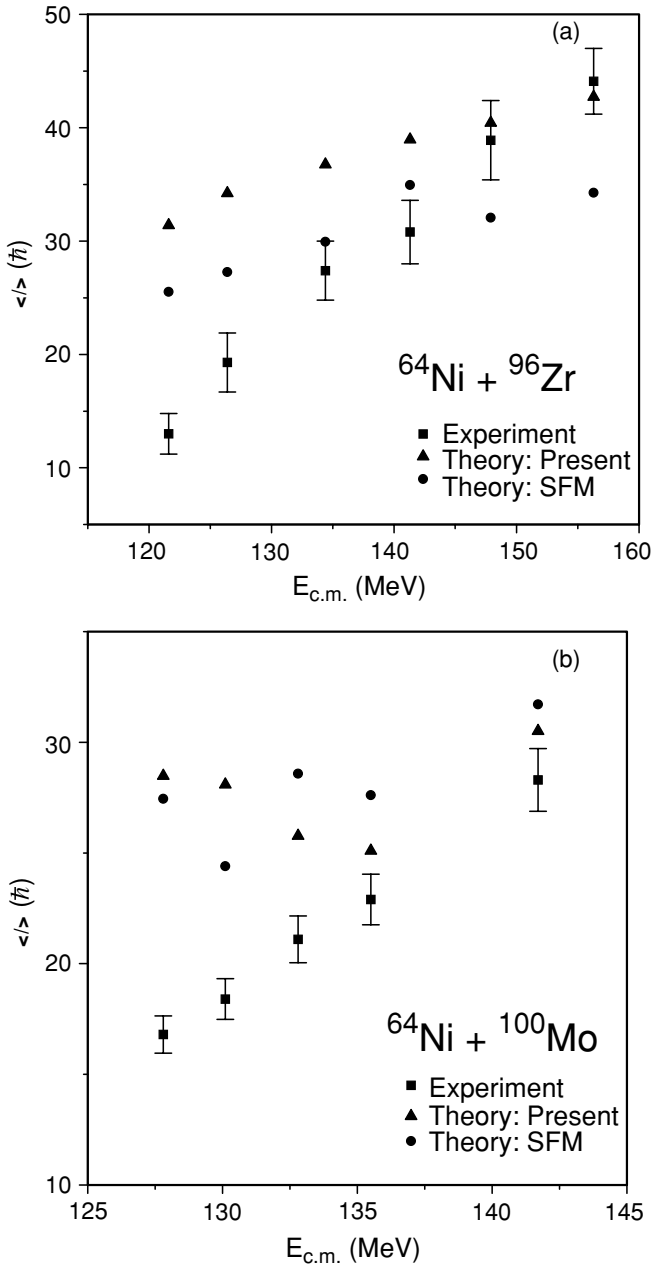

FIG. 4. Same as Fig 3, but for mean angular momentum.

parameter ($r_0 = 1.18$ fm). In Ref. [13], it was shown that a little change in r_0 has a drastic effects on the results. Our results were done with the standard Einstein relation.

We have proposed a Langevin equation for the description of heavy ion collisions. Contrary to the approach in Ref. [13], we were quite able to reproduce fusion cross sections at high energies and partially reproduce the mean angular momentum. The temperature is set to be zero at the initial position. The system evolves toward smaller r. The energy is transferred from the relative motion to the intrinsic one. If the energy loss from the relative motion exceeds $E_{\text{c.m.}} - B_f$ (B_f being the fusion barrier), when the system comes back to the fusion barrier, it is considered a fusion event. For s-wave scattering between $^{64}N_i$ and ^{100}Mo, the temperature T is 0.96 and 1.27 MeV for $E_{\text{c.m.}} = 127.8$ and 141.8 MeV, respectively. T is given by $T = \sqrt{\frac{E_{\text{c.m.}} - B_f}{a}}$ with $a = \frac{A}{8}$ the level density parameter. One may expect the collective parameters and their dependence on the temperature [14] to be the origin of the disagreement, but this cannot explain why we obtain good results for certain energies and bad ones for others; this question must be carefully examined. Alternatively, we were not able to reproduce both fusion cross sections with the standard parameters of SFM. Besides, the crucial quantity which is beyond the disagreement is a lower fusion barrier calculated with the Yukawa-plus-exponential method. We underline the fact that this potential must be revised. We note that the experimental fusion barrier corresponds to $E_{\text{c.m.}}$ for which $\sigma_F = 0$; for the energies 127.8 and 121.6 MeV, the

fusion cross sections are very weak compared to all other energies. If you diminish these energies by a few MeV, you will find $\sigma_F = 0$ [15–17]. We note that for $E_{\text{c.m.}} = 120$ MeV, σ_F is sensibly zero. We can see from the experimental cross sections ($\sigma_F = 0.26$ mb at $E_{\text{c.m.}} = 121.6$ MeV for ^{64}Ni+^{96}Zr) and ($\sigma_F = 0.38$ mb at $E_{\text{c.m.}} = 127.8$ MeV for ^{64}Ni+^{100}Mo) that the saddle potential V_f is around these values because σ_F is weak. We can give a rough estimate for $V_f =$ 120 MeV. The Yukawa-plus by exponential potential gives for the saddle potential $V_f = 102$ MeV for ^{64}Ni+^{96}Zr and $V_f = 109$ MeV for ^{64}Ni+^{100}Mo, which we find lower than the expected saddle potential. This explains why we find large cross sections at low energies. Also, if the fusion barrier is higher than the Yukawa-plus-exponential barrier, the critical angular momentum l_{crit} becomes lower and the mean fusion angular momentum diminishes for all energies, contrary to our finding.

ACKNOWLEDGMENTS

The authors thank Prof W. Helman and Dr. J. Hans for their valuable comments. This work is partially sponsored by M.E.R.S (Ministère de l'Enseignement et de la Recherche Scientifique): Contract No. D0701/01/04. This work is dedicated to Prof. J. Richert, Prof. N. Mebarki, and Prof. S. Hassani.

[1] P. Grangé, S. Hassani, H. A. Weidenmuller, A. Gavron, J. R. Nix, and A. J. Sierk, Phys. Rev. C **34**, 209 (1986).
[2] P. Frobrich, Phys. Rep. **116**, 337 (1984).
[3] D. H. E. Gross and H. Kalinowski, Phys. Rep. **45**, 175 (1978).
[4] J. Blocki, H. Feldmeier, and W. J. Swiatecki, Nucl. Phys. **A459**, 145 (1986).
[5] M. Brack, J. Damgaard, A. S. Jensen, H. C. Pauli, V. M. Strutinskii, and C. Y. Wong, Rev. Mod. Phys. **44**, 320 (1972).
[6] H. J. Krappe, J. R. Nix, and A. J. Sierk, Phys. Rev. C **20**, 992 (1979).
[7] J. Blocki, O. Mazonka, J. Wilczynski, Z. Sosin, and A. Wieloch, Acta Phys. Pol. B **31**, 1513 (2000).
[8] W. D. Myers and W. J. Swiatecki, Nucl. Phys. **81**, 1 (1966).
[9] I. Kelson, Phys. Rev. B **136**, 1667 (1964).
[10] J. Blocki, J. Randrup, W. J. Swiatecki, and C. W. Tsang, Ann. Phys. (NY) **105**, 427 (1977).
[11] A. M. Stefanini, L. Corradi, D. Ackermann, A. Facco, F. Gramegna, H. Moreno, L. Meuller, D. R. Napoli, G. F. Prete, P. Spolaore, S. Beghini, D. Fabris, G. Montagnoli, G. Nebbia, J. A. Ruiz, G. F. Segato, C. Signorini, and G. Viesti, Nucl. Phys. **A548**, 453 (1992).
[12] M. L. Halbert, J. R. Beene, D. C. Hensley, K. Honkanen, T. M. Semkow, V. Abenante, D. G. Sarantites, and Z. Li, Phys. Rev. C **40**, 2558 (1989).
[13] W. Przystupa and K. Pomorski, Nucl. Phys. **A572**, 153 (1994).
[14] K. Pomorski and H. Hofmann, Phys. Lett. **B263**, 164 (1991).
[15] D. Boilley, Y. Abe, and J.-D. Bao, Eur. Phys. J. A **18**, 627 (2003).
[16] W. J. Swiatecki, K. Siwek-Wilczynska, and J. Wilczynski, Acta Phys. Pol. B **34**, 2049 (2003).
[17] W. J. Swiatecki, K. Siwek-Wilczynska, and J. Wilczynski, Phys. Rev. C **71**, 014602 (2005).